COMPRESSOR ROTOR AERODYNAMICS

Robert P. Dring, Manager Gas Turbine Technology
H. David Joslyn, Research Engineer
Joel H. Wagner, Research Engineer
United Technologies Research Center
East Hartford, Connecticut 06108 U.S.A.

SUMMARY

Although the numerical sophistication of multi-stage turbomachinery through-flow calculations has evolved to a very high level, the aerodynamic inputs of total pressure loss, deviation and blockage are subject to a high degree of empiricism. There is a need for detailed flow field data in a multi-stage environment in order to bring some discipline to this important aspect of turbomachinery design. This paper presents a survey of some of the initial results of an in-depth investigation of the aerodynamics of the second stage of a large scale two-stage axial compressor. The second stage rotor data will be compared with data obtained on an isolated rotor with very thin and then very thick inlet hub and tip boundary layers. The single and multi-stage rotor data presented here include surface flow visualization and rotating frame radial/circumferential traverse measurements presented in the form of fullspan contour plots of rotary total pressure. Also presented are the spanwise distributions of loss, deviation and blockage. Some implications of these results for through-flow analyses are discussed.

INTRODUCTION

The "through-flow" analysis in compressor (and turbine) design is a two-dimensional, axisymmetric calculation describing the spanwise variation of the flow at streamwise locations both within and between blade rows from the inlet of the compressor to its discharge. The analysis is used both to determine rotor and stator metal angles for optimum design point performance (based on various criteria for optimum incidence and deviation) and to predict off-design performance and the approach to stall or choking. It is a fairly well recognized fact that the limiting feature in the accuracy of a through-flow analysis is not so much in the numerics but rather in the aerodynamic data that the analysis requires as input. This observation has also been made in at least two prior AGARD reports (Refs. 1 and 2). Specifically, it was observed that there "was a lack of reliable and publicly available data especially for multi-stage compressors".

In recognition of this state of affairs, since 1977 the UTRC Large Scale Rotating Rig (LSRR) has been engaged in obtaining detailed data of high quality in the flows over isolated compressor rotors and in a multi-stage compressor environment. The objectives of this program include (1) gaining a better physical understanding and providing a basis for improved analytical models for the complex three-dimensional flows present in compressor blade rows, and (2) conducting detailed comparisons between measured and computed results both on a blade-to-blade basis and on a through-flow basis. To date this combined experimental and analytical program has included: (1) an isolated rotor with thin inlet boundary layers ($\delta \approx$ 5 to 10% span) on the hub and casing (Refs. 3 and 4), (2) the same rotor with thick inlet boundary layers ($\delta \approx$ 37% span) on the hub and casing (Ref. 5), and (3) a two stage compressor. Each one of these test programs includes a large amount of detailed, high quality data taken on the airfoils and in the flows downstream of the airfoils.

This paper presents a survey of some of the results obtained in these three test programs. The data to be presented for each of the three rotor tests includes: surface flow visualization on the airfoil and on the endwall, rotating frame radial-circumferential traverse measurements presented in the form of fullspan contour plots of rotary total pressure, and spanwise distributions of mass averaged total pressure loss, inlet and exit flow angle and blockage. The results for the three rotors will be compared and their implications so far as through-flow analyses are concerned will be discussed.

Of particular significance in this regard is the concept of blockage. Considering its pivotal role in compressor through-flow analysis, blockage has been the subject of remarkably little discussion in the literature. The concept of blockage is an empirical attempt on the part of the compressor analyst to account for the difference in a through-flow analysis between mass averaged quantities (such as work) and area averaged quantities (such as mass flow). Historically, blockage has been based on rough estimates reflecting past experience and little or no direct physical measurement. It has been deduced analytically from previous compressor test results. Errors in estimated blockage are one of the primary reasons for compressors initially not achieving their design goals of flow, pressure rise and efficiency.

Because of the highly detailed nature of the results that can be obtained in both the rotating and stationary frames of reference in the UTRC LSRR blockage can be calculated directly from the data. The results clearly indicate the sites and magnitudes of the major

contributions to blockage (i.e., corner stall and casing boundary layer flow) and, as such, they provide a unique basis for an analytical explanation and representation of this phenomena.

EXPERIMENTAL FACILITY AND INSTRUMENTATION

The United Technologies Research Center Large Scale Rotating Rig (LSRR) is 5-ft (1.52 m) in diameter and can run at speeds up to 900 rpm. The inlet flow is from ambient room air and the flow through the facility is essentially incompressible. More detailed descriptions of the rig and its data acquisition system are available in Refs. 4 and 6.

The airfoil geometry and the aerodynamic test conditions for both the isolated compressor rotor and the two stage compressor rotor are summarized in Table I. The isolated rotor had a 6 inch (0.152 m) chord (B) and was tested both with thin inlet hub and casing boundary layers (δ_{hub} = 5% span and δ_{tip} = 10% span) and with thick inlet hub and casing boundary layers ($\delta_{hub} = \delta_{tip}$ = 37% span). The results of these two test programs are presented in detail in Refs. 3 and 4 for the thin case and in Ref. 5 for the thick case. The absolute inlet flow in both cases was axial. The second stage rotor tested in the two stage compressor had a 4 inch (0.102 m) chord and its inlet conditions were determined by the flow leaving the first stage stator.

The present discussion is limited to the data taken when both rotors were being operated at their nominal design flow coefficients (ϕ). These are 0.85 for the isolated rotor and 0.51 for the two stage rotor. These flow coefficients are based on the area averaged C_x and the wheel speed at midspan (U_m). The flow coefficients that will be quoted for the isolated rotor with the thin inlet boundary layer will be based on midspan C_x at the inlet which is 2 percent greater than the area average. This is done in order to be consistent with all of the results presented in Refs. 3 and 4 where the inlet midspan C_x was used.

The major differences between the isolated and two stage rotors are in their nominal design flow coefficients (0.85 and 0.51), their stalling flow coefficients (approximately 0.6 and 0.44), their aspect ratios (1.0 and 1.5) and their tip clearance to chord ratios (0.016 and 0.039).

The technique used to obtain the airfoil and endwall surface flow visualization has been discussed and demonstrated previously in Refs. 3, 4, 5 and 6. In brief, it consisted of seeping a small amount of ammonia out of one of the airfoil surface static pressure taps. The ammonia caused a dark blue streak line to form on Ozalid paper attached to the surface downstream of the pressure tap. The technique is particularly well suited to the rotating frame of reference.

The rotating frame radial-circumferential traverse system has also been described earlier in Refs. 4 and 6 and is shown in some detail in Ref. 3. The device can traverse circumferentially over two blade pitches and radially from hub to tip. In the present programs data was acquired from 5 percent span to 97 percent span. The traverse can be located at various positions ($\Delta X/B_X$) downstream of the rotor (as in Ref. 4). For the present program, however, at midspan the traverse was 30 percent of the rotor axial chord axially downstream of the isolated rotor. For the two stage rotor it was located 25 percent downstream, midway between the rotor trailing edge and the second stator leading edge. These locations were chosen based on mechanical constraints (i.e., the two stage rotor-stator axial gap) and on aerodynamic constraints. Aerodynamically it was desirable to have the traverse close to the trailing edge to show detail in the flow and not so close as to be in any locally stalled region as occurred for the isolated rotor at a traverse location only 10 percent downstream (Ref. 4).

The traverse probe used was a United Sensor five hole probe (USC-F-152) modified to include a cobra probe for traversing very close to the hub. The probe tip was small relative to the flow field (Dia. = 0.093 inches, 2.4 mm). The probe was operated in a computer controlled yaw nulling mode. Data was acquired at approximately 20 radial locations and at typically 50 circumferential locations for 1000 measurement sites per plane. Measurement locations were concentrated in the hub and tip endwall regions and in the airfoil wake.

FLOW VISUALIZATION

The results of the surface flow visualization will be discussed first, before any of the detailed traverse data, in order to provide some physical insight into the nature of the flows in the three rotor tests. Generally speaking there were many very similar features in the three flow visualization results (Figs. 1, 2 and 3). The suction surfaces were very nearly two-dimensional in nature over much of their area. The major departure from two-dimensionality is the corner stall region present in all three tests.

The corner stall region for the two isolated rotor tests (thin and thick inlet boundary layers) are very similar in size and shape. The flow in the stalled region is generally outward (toward the tip) and there is a region of reversed flow out to about 25 percent span. The corner stall region begins slightly downstream of midchord and it displaces the profile boundary layer outward (toward the tip) to about midspan (a distance of about 50% chord from the endwall). The corner stall region on the two stage rotor was slightly

smaller, starting slightly aft of midchord, but it displaced the profile boundary layer outward a distance somewhat larger than half the chord. Note that these comparisons of the nature of the corner stall region are at the nominal design flow coefficients and that their spanwise and chordwise extent will be a strong function of loading (Ref. 4). The spanwise extent of the corner stall region will depend on the relative "health" of the suction surface boundary layer above it. The spanwise extent will increase as boundary layer separation is approached. Low momentum fluid in the hub stall regions tends to be centrifuged toward the tip and can eventually reach the tip (Ref. 4).

The tip region of the suction surface has a weak outflow due to the leakage flow over the tip entraining the suction surface flow. There is, however, no evidence of a strong suction surface corner stall at the tip. This is consistent with the results of Ref. 7 (Plate 5) where it was observed that the tip clearance flow tends to "wash away" the corner stall. It was observed in Ref. 7 that a clearance to chord ratio of 0.04 was optimum in terms of minimizing the extent of the corner stall region. This is very close to the relatively large clearance to chord ratio of the two stage rotor (Table I).

The pressure surfaces of the three rotors were very nearly two dimensional (collateral) over most of the airfoil. The radial component of surface flow was small except in the immediate vicinity of the tip. Here there was a weak radial outflow due to leakage and no indication of a scraping vortex (i.e., flow toward the hub).

On the hub the effects of secondary flow in the endwall boundary layer were minimal. The endwall flows were nearly collateral with a trajectory close to the airfoil mean camber line. The corner stall region had no significant impact on the hub endwall boundary layer.

In conclusion, the flow visualization results indicate that the major departures from what would be otherwise highly two-dimensional boundary layer flow, are due to the corner stall region at the hub and to the leakage flow at the tip.

CONTOURS OF ROTARY TOTAL PRESSURE

Contour plots of rotary total pressure measured in the flow downstream of the three rotors are shown in Figs. 4, 5 and 6. The data for the isolated rotor with the thin inlet boundary layers covers 1.32 pitches. The data for the thick inlet boundary layer and for the two stage rotor covers two pitches. Recall that for the two isolated rotor tests the traverse plane was 30 percent aft of the rotor and that for the two stage test it was 25 percent aft. In all cases the suction surface side of the wake is to the left and the pressure surface side of the wake is to the right.

Rotary total pressure is defined as follows:

$$P_{T,rot} \equiv P + \tfrac{1}{2}\rho(W^2-U^2) = P_{T,abs} - \rho U C_\theta \qquad (1)$$

where W, U and C_θ are the relative flow speed, the wheel speed and the absolute swirl velocity, respectively. Rotary total pressure was chosen for the present discussions since (unlike relative total pressure) for inviscid flow it is invariant with radius change along a stream line in the rotating frame of reference. It is also desirable to look at rotary total pressure from the point of view of secondary flow. For flow with uniform density, gradients in rotary total pressure are the driving potential for secondary flow in the rotating frame of reference in the same manner as gradients in absolute total pressure are the driving potential for secondary flow in the stationary frame of reference (Ref. 8). The increment between the values of the rotary total pressure on the various contours has been normalized by a dynamic pressure based on wheel speed at midspan.

For the isolated rotor with the thin inlet boundary layer (Fig. 4) there is a large "free stream" region of constant rotary total pressure between the wakes and the endwalls. This is present due to the thinness of the inlet boundary layers (δ = 5 and 10% span) and the constant absolute total pressure in the inlet core flow region. The contours for the isolated rotor with the thick inlet boundary layers (Fig. 5) are quite different. The circumferential contours in the free stream region between the wakes and the endwalls are due to the radial gradients in absolute total pressure in the thick boundary layers (δ = 37% span) in the fluid entering the rotor. For the two stage rotor (Fig. 6) the contours in the free stream region are due to the upstream inlet guide vane, rotor and stator. Comparatively speaking, however, the flow in the free stream region has a relatively uniform rotary total pressure. In general, many of the same features can be seen in varying magnitude in all three rotor exit flow fields.

At the hub, the data for both isolated rotor tests (Figs. 4 and 5) show little evidence of Bernoulli surface rotation due to secondary flow. The streamwise component of vorticity generated by turning the flow is insufficient to overcome the initial inlet streamwise vorticity. The former would move endwall fluid from the pressure to the suction surface side of the channel while the latter (due to inlet skewing) tends to drive the endwall boundary layer fluid toward the pressure surface (Ref. 9). There is some indication of flow toward the hub on the pressure surface side of the passage. Finally, for both isolated rotor cases there is a thickening of the blade wake in the hub region due to the corner stall. The thickening for the thin and thick cases is very similar. This observation is

consistent with those of Ref. 10 where it was demonstrated that the severity of the corner stall was insensitive to the thickness of the inlet boundary layer.

The data for the two stage rotor (Fig. 6) indicated that the flow in the hub region was relatively clean, that is, similar to the isolated rotor with the thin inlet boundary layer in that no strong shear regions were evident. There is some evidence of Bernoulli surface rotation due to secondary flow near the suction surface. The corner stall region is very thin relative to those of the two isolated rotor cases and appears as little more than a thickening of the blade wake. The corner stall begins to deepen and thicken the wake at about midspan.

From the hub region the following conclusions can be drawn. The corner stall is the major source of hub loss and blockage. The corner stall behaves more like a thickened blade wake rather than a thickening of the hub endwall boundary layer. Finally, for the two isolated rotor cases, the effects of secondary flow were minimized due to the skewing and energizing of the hub boundary layer as it comes onto the rotating hub.

When comparing the flows in the tip region recall that the clearance for the two isolated rotor tests was 1.6 percent of chord while for the two stage test it was 3.9 percent of chord. The flow in the tip regions is influenced by tip leakage, wall motion (toward the pressure surface) and the inlet boundary layer. For the two isolated rotor cases (Fig. 4 and 5) the low total pressure region is nearly midway between adjacent airfoil wakes. This is similar to results presented for tip leakage in a stationary cascade without an endwall present and with a clearance to chord ratio of 4 percent (Ref. 7, experiments A and B).

The tip region of the two stage rotor was considerably different in that the low total pressure region was very close to the pressure surface. For this case the center of the low total pressure region was located 30 percent further from the tip endwall, inspite of the shorter chord. These differences must in some measure be due to the much larger tip clearance of the two stage rotor.

ROTOR TOTAL PRESSURE LOSS

One of the more significant pieces of information to be derived from the traverse data presented above is the spanwise distribution of the rotor total pressure loss. In the present discussion the total pressure loss coefficient ($C_{PT,rel}$) is defined as the difference between the mass averaged inlet and exit relative (or rotary) total pressures at a fixed radius, normalized with a dynamic pressure based on the wheel speed at midspan. Strictly speaking the total pressure difference should be taken along a fixed (axisymmetric) stream surface. For all three rotors the maximum radial displacement of a stream surface was about 1 percent span (near midspan). Finally, the mass averaging of the total pressures was based on the measured circumferential distributions of flow speed, yaw and pitch from which the local C_x could be calculated.

The data for the thin and thick inlet boundary layer tests on the isolated rotor are shown in Fig. 7. For the thin case, since the rotary total pressure is constant over the core flow at inlet radial shifting of the stream surfaces is of no consequence in computing the net loss. In fact, for this case the inlet boundary layer only affected the loss at the two or three data points closest to the endwalls. The corner stall region (Fig. 1) and the low rotary total pressure region associated with it (Fig. 4) have caused a loss level which is very high relative to two-dimensional (profile) loss levels and which penetrates out to 40 percent span. The high loss region at the tip is felt from 75 percent span outward. The loss in the midspan region is representative of two-dimensional cascade levels (Ref. 4, Fig. 6).

For the isolated rotor with the thick inlet boundary layers (Fig. 7) there is a region of very low loss out to 10 percent span due to the weak radial redistribution of the inlet rotary total pressure profile. As mentioned above, high total pressure fluid moved toward the hub near the pressure surface side of the wake (Fig. 5) causing an increase in rotary total pressure in the region and hence a local reduction to the mass averaged loss. Similar effects can be seen in the cascade results of Ref. 7 (Fig. 21) and in the rotating rig data of Ref. 11 (Fig. 6) where spanwise redistribution of high and low total pressure fluid caused a negative mass averaged total pressure loss near the endwalls. These observations regarding endwall flow in compressor airfoil passages and the dominant contributions of corner stall relative to endwall secondary flow are consistent with similar observations made in Ref. 10.

The thick inlet boundary layer isolated rotor test indicated no well defined low loss region at midspan as occurred for the thin case. Both the hub and tip high loss regions occupied a larger portion of the span than in the thin case. The reason for this difference is not evident in the flow visualizations (Figs. 1 and 2) but it is somewhat suggested by the rotary total pressure contours (Figs. 4 and 5).

The loss data for the two stage rotor is presented in Fig. 8. The radial distribution of the rotor inlet relative total pressure was computed by mass averaging the circumferential distributions of relative total pressure computed from the absolute frame traverse data taken at the first stator exit. The nature of the loss distribution near the hub is similar to that of the thick inlet boundary layer isolated rotor tests, with a low (negative) loss region close to the endwall. Here, as above, the low and negative loss region

at the hub is due to the high total pressure fluid moving toward the hub near the pressure surface side of the blade wake (Fig. 6).

In the midspan region the loss level is slightly negative (1.3% at midspan). There are a number of possible explanations for this result, any one or all of which may be contributing to the negative loss. (1) It may be a result of experimental error. An error of 0.5 percent in the measured total pressure at the rotor inlet and at the rotor exit could account for the negative loss. (2) The negative loss could actually be present due to a radial redistribution of high and low total pressure fluid such as occurred near the hub. (3) The negative loss is in part due to a radial shift of the axisymmetric stream surfaces between the rotor inlet and exit measurement planes. This is possible due to the relatively large radial gradient in rotary total pressure in the midspan region of the flow. The radial shift of slightly more than 1 percent span between rotor inlet and exit is sufficient to explain half of the negative loss at the 40 percent span location where it is maximum.

FLOW ANGLES

The rotor inlet and exit metal angles (θ^*) and the inlet and exit flow angles (θ) are presented in Figs. 9 and 10. For the two isolated rotor cases the inlet flow angles were calculated from wheel speed and the measured radial variation of C_x. The inlet flow angle for the two stage rotor is based on mass averaged relative flow angles calculated from the stationary frame measurements made at the first stator exit. The rotor exit flow angles were measured in the rotating frame of reference and mass averaged based on the circumferential distributions of flow angle and C_x. Mass averaging reduces the impact of the nearly axial flow in the low velocity region immediately downstream of the corner stall.

Since both isolated rotor tests (thin and thick inlet boundary layers) were run at the same flow coefficient based on area averaged C_x the thin case was running closer to the stall from 20 percent span to 80 percent span. In the endwall regions the thick case was running closer to stall, causing the hub and tip boundary layers at the rotor inlet to be more heavily skewed in the direction opposing secondary flow due to turning. Aside from a shift in level (of approximately 2^o) the exit angle profile was relatively insensitive to inlet boundary layer thickness. The 2^o drop in deviation for the thick inlet boundary layer case is in part due to its lower inlet angle over the midspan region.

The large under turning in the tip region of both isolated rotor cases is due to at least three mechanisms. (1) Tip leakage contributes to the under turning. This was shown in Ref. 7 for a cascade and in Ref. 11 (Fig. 3) for a large scale multistage rotor. (2) Wall motion also contributes to the under turning. As the wall is approached the flow angle must approach 90^o. Finally (3) the inlet boundary is skewed toward the rotor pressure surface due to the rotor motion, leading to under turning.

The flow angle data for the two stage rotor in Fig. 10 are similar in many ways to the isolated rotor data. There is over turning at the hub due to corner stall and under turning at the tip due to leakage and wall motion. The results are also very similar to those of Ref. 11 (Fig. 3).

BLOCKAGE

Through-flow analyses are axisymmetric calculations of the radial distributions of mass averaged quantities. Mass flow (M), however, is related to the area average of ρC_x. The mass averaged quantities are related to this area average in the continuity equation by the blockage factor ($\bar{K}$).

$$M = 2\pi \int_{r_h}^{r_t} \bar{K} \rho \bar{C}_x^{PT} \, r \, dr \tag{2}$$

According to this expression $\bar{K}$ is the ratio of the area averaged axial velocity (or $\bar{C}_x^a$) to $\bar{C}_x{}^{PT}$, the axial velocity based on the mass averaged total and static pressures and the mass averaged yaw (θ) and pitch (ϕ) angles. This relationship may be expressed as follows.

$$\bar{K} \equiv \left(\bar{C}_x^a / \bar{C}_x^{PT} \right) = f(r) \tag{3}$$

where (for incompressible flow)

$$\bar{C}_x^{PT} \equiv \left(\sqrt{\bar{P}_T^m - \bar{P}_S^m / \tfrac{1}{2}\rho} \right) \cos \bar{\theta}^m \cos \bar{\phi}^m \tag{4}$$

In this notation (-a) indicates an area average and (-m) indicates a mass average. The description of blockage as a function of radius is consistent with what is referred to as "tangential" blockage in Ref. 2 (p. 329). It reflects all departures from axisymmetry from hub to tip including profile wakes, corner stall, tip leakage and so on. "Endwall" block-

age does not reflect a departure from axisymmetry but rather the inability of a small number of computational stream tubes to accurately account for the endwall boundary layers. Endwall blockage reflects the computational approach of coupling a through-flow calculation to an endwall boundary layer calculation. For example, endwall blockage would not be required in the single pass axisymmetric analysis of Ref. 12 which simultaneously solves both the viscous and inviscid regions of the flow. For this approach endwall blockage is unnecessary and only tangential blockage would be required.

Blockage distributions have been calculated from the measured data according to the above definition. They reflect the departure from axisymmetry from the hub to the tip, i.e., the fullspan distribution of tangential blockage. The major contribution to blockage for these three rotor test cases came from the total pressure. The area and mass averages of the static pressure and the yaw and pitch angles were generally very close to one another.

Recall that the traverse planes for the isolated rotor and for the two stage compressor are 30 percent and 25 percent respectively aft of the rotors. This is significant since blockage will be a strong function of distance downstream due to wake mixing.

The blockage distributions for the two isolated rotor tests are shown in Fig. 11. The spanwise variations are very similar to the spanwise variation of total pressure loss (Fig. 7). The similarity in blockage profiles is particularly interesting in view of the factor of 4 difference in the inlet boundary layer thickness for the two cases. The blockage data also points to the dominant role of corner stall relative to secondary flow and to the insensitivity of corner stall to inlet boundary layer thickness. The blockage profile for the two stage rotor is generally lower in the endwall regions than either of the two isolated rotor cases, even with the much larger relative tip clearance.

In conclusion, the blockage profiles bear a qualitative similarity to the loss profiles with the major contributions being due to hub corner stall and tip endwall and leakage flow. The midspan blockage for all three cases (at their nominal design flow coefficients) is very small.

CONCLUSIONS

This paper has presented a comparison of several types of data acquired on three compressor rotor configurations: an isolated rotor with very thin inlet hub and tip boundary layers, the same rotor with thick inlet boundary layers, and a two stage compressor second stage rotor, each running at its nominal design flow coefficient. The data examined for each configuration consisted of surface flow visualization, a radial-circumferential distribution of rotary total pressure in the flow aft of the rotor, and the spanwise distribution of loss, flow angle and blockage.

There were many strong similarities in the main features of the flow over the three rotors. The most striking was the strong influence of hub corner stall (as opposed to the hub endwall boundary layer) on the loss, deviation and blockage and its insensitivity to inlet boundary layer thickness. The tip boundary layer and leakage flow were also seen to have a strong impact. Although secondary flow was generally seen to be rather weak, as evidenced by the slight rotation of the Bernoulli surfaces and the lack of cross flow in the hub boundary layers, radial redistribution of high and low total pressure fluid through the rotor passage and in the downstream flow was observed to produce spanwise distributions of the total pressure loss which were locally negative. This radial redistribution could have been due to mechanisms other than the weak secondary flow, e.g., it could have been a result of the radial outflow in the corner stall region.

The present two stage compressor program is being continued with particular emphasis in the areas of tip clearance effects, off-design performance and the stator. As a result of these and the earlier experimental studies and companion analytical work it is expected that a more complete and detailed understanding of multi-stage compressor aerodynamics will emerge.

REFERENCES

1. -----, AGARD Conference Proceedings No. 195 on Through-Flow Calculations in Axial Turbomachinery, 47th meeting of AGARD/PEP, AGARD-CP-195, May 20-21, 1976.
2. -----, AGARD Advistory Report No. 175, Propulsion and Energetics Panel Working Group 12 on Through-Flow Calculations in Axial Turbomachines, AGARD-AR-175, October 1981.
3. Dring, R, P., H. D. Joslyn and L. W. Hardin: "Experimental Investigation of Compressor Rotor Wakes," AFAPL-TR-79-2107, Air Force Aero Propulsion Laboratory, Technology Branch, Turbine Engine Division (TBX), Wright-Patterson Air Force Base, OH.
4. Dring, R. P., H. D. Joslyn and L. W. Hardin: "An Investigation of Compressor Rotor Aerodynamics," ASME, Journal of Engineering for Power, January 1982, Vol. 104, p. 84-96.
5. Wagner, J. H., R. P. Dring and H. D. Joslyn: "Axial Compressor Middle Stage Secondary Flow Study," final report submitted to NASA-Lewis Research Center for Contract No. NAS3-23157, December 1982.
6. Dring, R. P. and H. D. Joslyn: "Measurements of Turbine Rotor Blade Flows," ASME Gas Turbine Conference, New Orleans, LA, Measurement Methods in Rotating Components of Turbomachinery, p. 51-58.
7. Lakshminarayana, B. and J. H. Horlock: "Leakage and Secondary Flows in Compressor Cascades," ARC, R&M No. 3483, 1967.
8. Hawthorne, W. R.: "Secondary Vorticity in Stratified Compressible Fluids in Rotating Systems," CUED/A-Turbo/TR 63, University of Cambridge, England, 1974.
9. Moore, R. W. and D. L. Richardson: "Skewed Boundary Layer Flow Near the Endwalls of a Compressor Cascade," Trans. ASME, Vol. 79, November 1957.
10. Horlock, J. H., J. F. Louis, P. M. E. Percival and B. Lakshminarayana: "Wall Stall in Compressor Cascades," Trans. ASME, Journal of Basic Engineering, Vol. 88, September 1966, pp. 637-648.
11. Adkins, G. G. and L. H. Smith: "Spanwise Mixing in Axial-Flow Turbomachines," ASME, Journal of Engineering for Power, January 1982, Vol. 104, p. 97-110.
12. Anderson, O. L.: "Calculation of Internal Viscous Flows in Axisymmetric Ducts of Moderate to High Reynolds Numbers," Computers and Fluids, Vol. 8, p. 391-411, 1980.

ACKNOWLEDGEMENTS

The thin boundary layer isolated rotor data was acquired partially under Air Force contract funding under the direction of C. Herbert Law (AFWAL/POTX), project engineer, Contract Number F33615-77-C-2083, and partially under UTRC corporate funding. The thick boundary layer isolated rotor data was acquired under funding from NASA Lewis Research Center under the direction of Mr. Michael Pierzga, project manager, Contract Number NAS3-23157. The two stage compressor is being tested under PWA and UTRC corporate funding.

TABLE I - ROTOR GEOMETRY & TEST CONDITIONS

	Isolated Rotor	Two-Stage Rotor
Number of Airfoils	28	44
τ_m/B	1.01	0.97
Span/B	1.00	1.50
Clrnc/B	0.016	0.039
α_s	35.5^o	47.1^o
Camber	49^o	35^o
Hub/Tip	0.8	0.8
N (rpm)	510	650
$\bar{C}_x$ (f/s)	102	78
Re (W_1,B)	4.9×10^5	3.0×10^5
ϕ	0.85	0.51
$(\Delta X/B_x)$	0.30	0.25

Figure 1 Isolated Rotor, Thin Inlet Boundary Layers, Suction Surface, $\phi = 0.85$

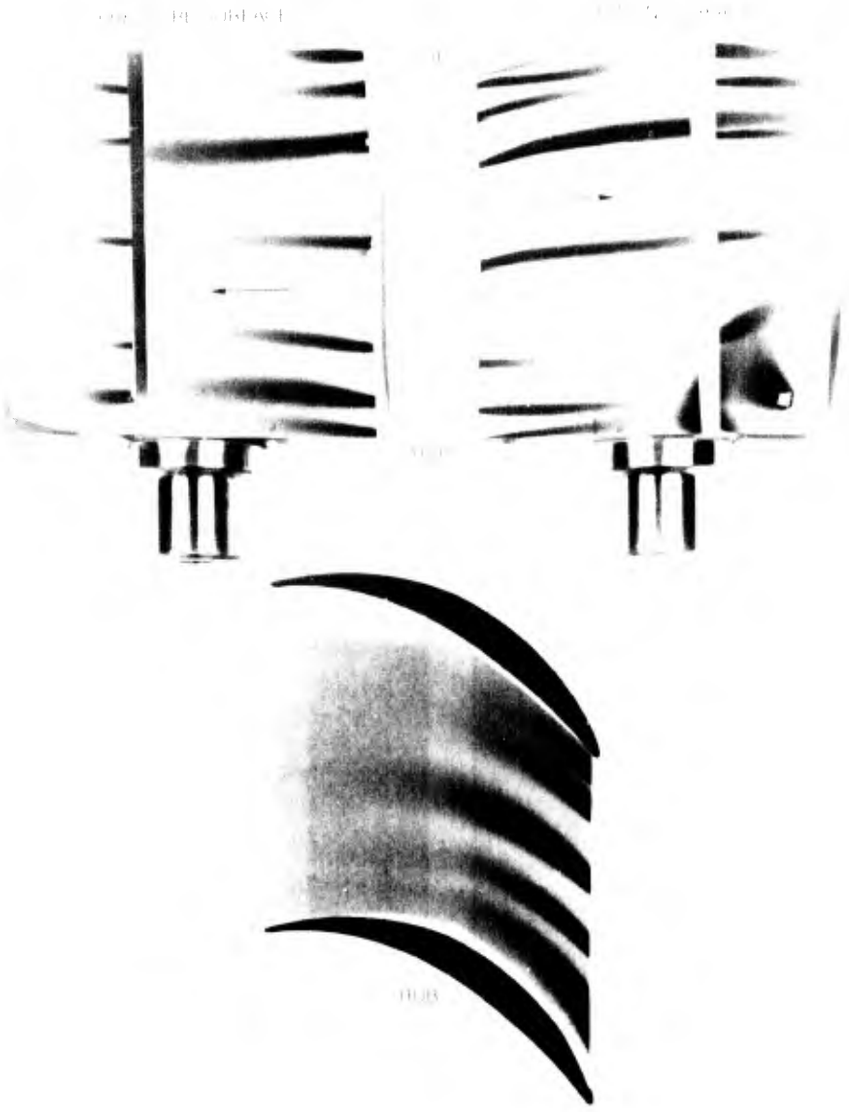

Figure 2 Isolated Rotor, Thick Inlet Boundary Layers, $\gamma = 0.85$

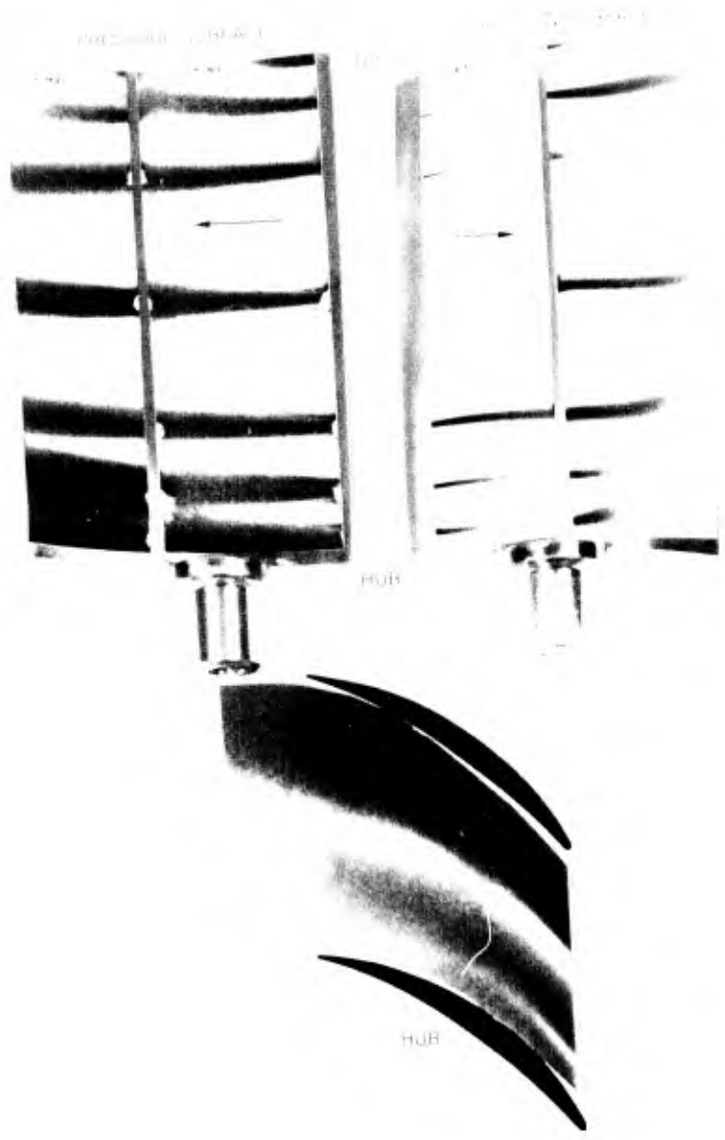

Figure 3 Two Stage Compressor, Second Stage Rotor, $\lambda = 0.51$

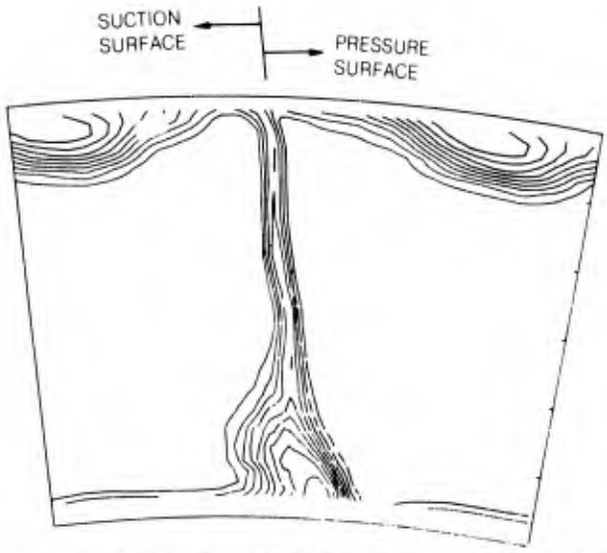

Figure 4 Isolated Rotor, Thin Inlet Boundary Layers, Rotary Total Pressure, ϕ = 0.85, 30% aft, 1.32 Pitches, ΔC_{pT} = 0.1

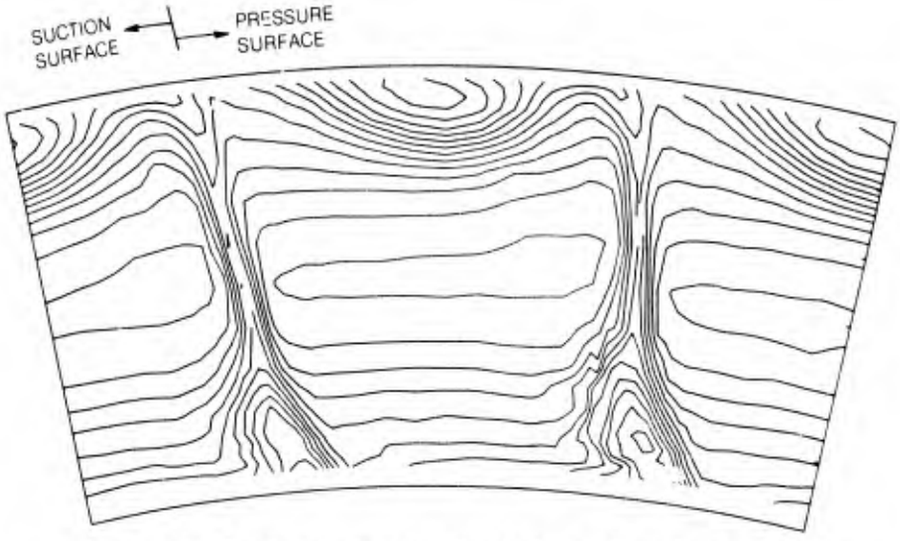

Figure 5 Isolated Rotor, Thick Inlet Boundary Layers, Rotary Total Pressure, ϕ = 0.85, 30% aft, 2.0 pitches, ΔC_{pT} = 0.1

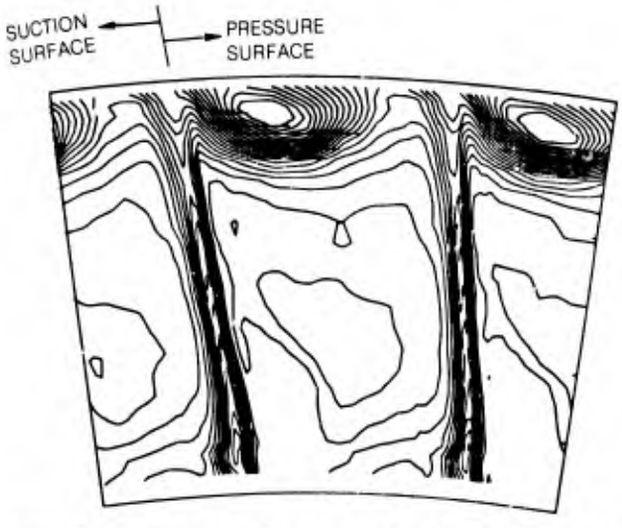

Figure 6 Two Stage Compressor, Second Stage Rotor, Rotary Total Pressure, ϕ = 0.51, 25% aft, 2.0 pitches, ΔC_{pT} = 0.025

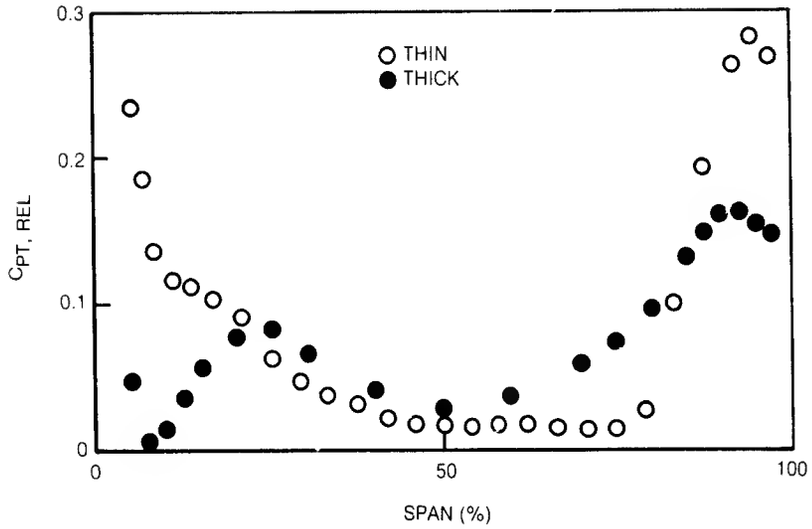

Figure 7 Isolated Rotor, Thin and Thick Inlet Boundary Layers, Total Pressure Loss, $\phi = 0.85$

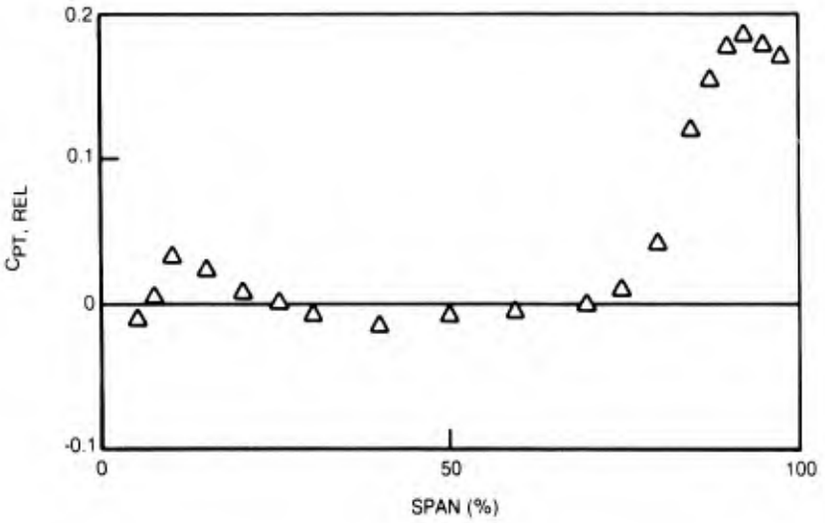

Figure 8 Two Stage Compressor, Second Stage Rotor, Total Pressure Loss, $\phi = 0.51$

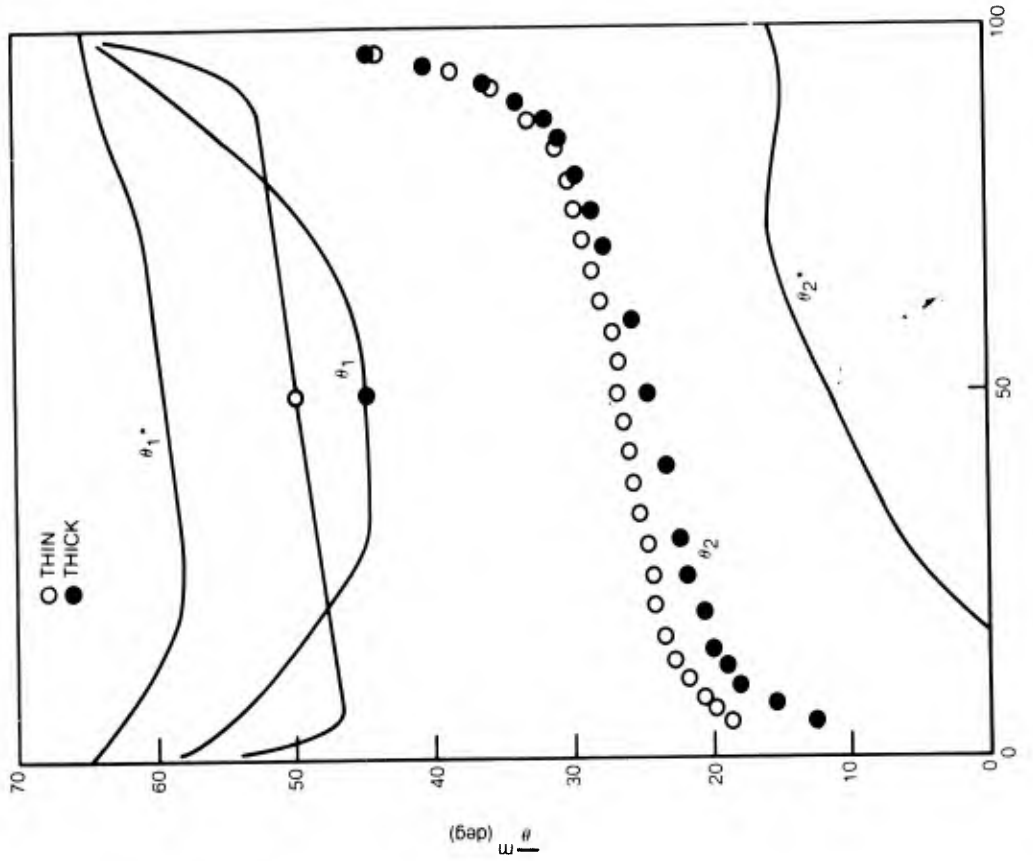

Figure 9 Isolated Rotor, Thin and Thick Inlet Boundary Layers, Relative Flow Angels, $\phi = 0.85$

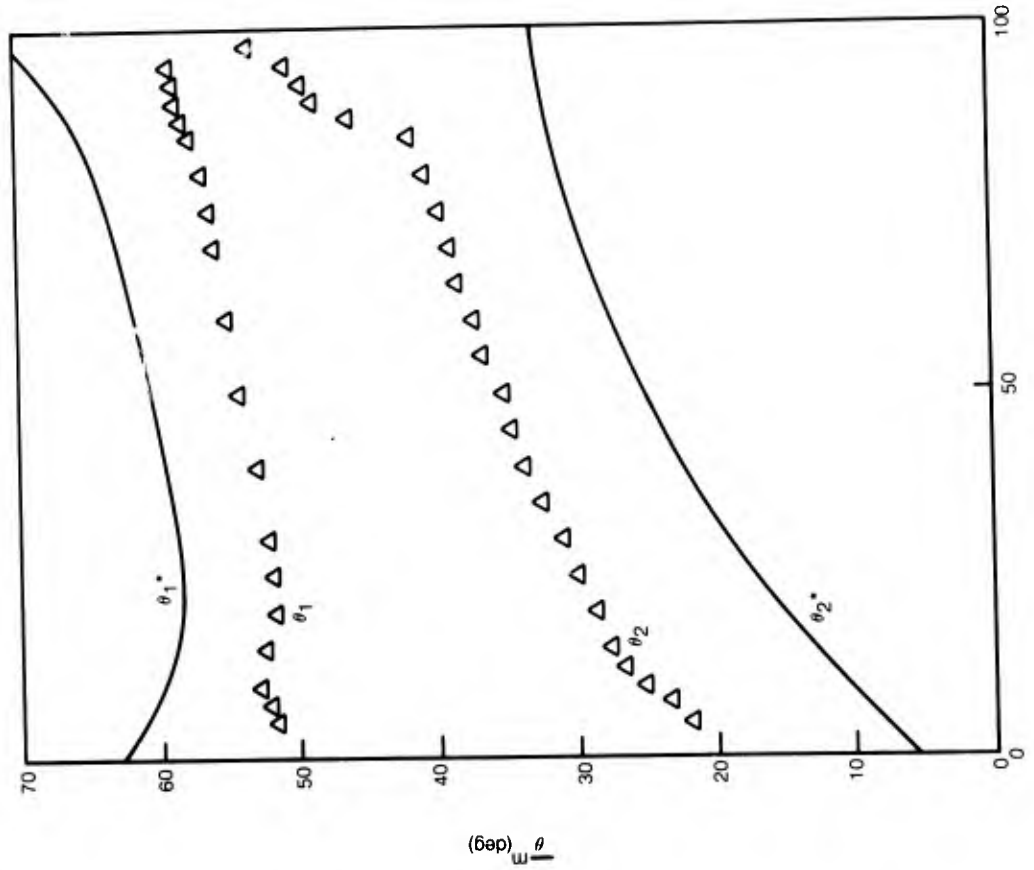

Figure 10 Two Stage Compressor, Second Stage Rotor, Relative Flow Angles, $\phi = 0.51$

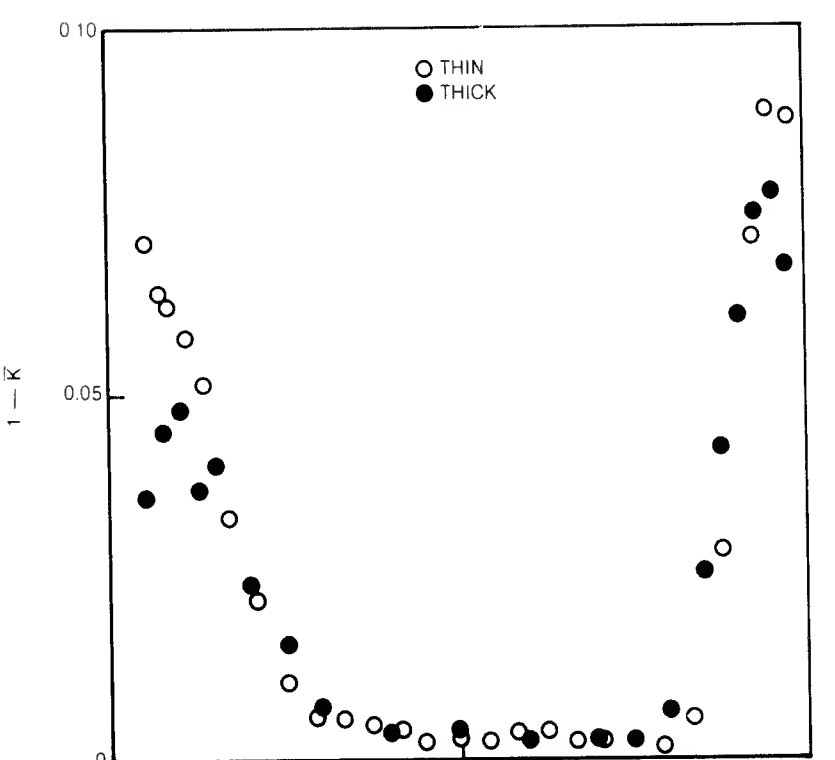

Figure 11 Isolated Rotor, Thin and Thick Inlet Boundary Layers, Blockage, ϕ = 0.85

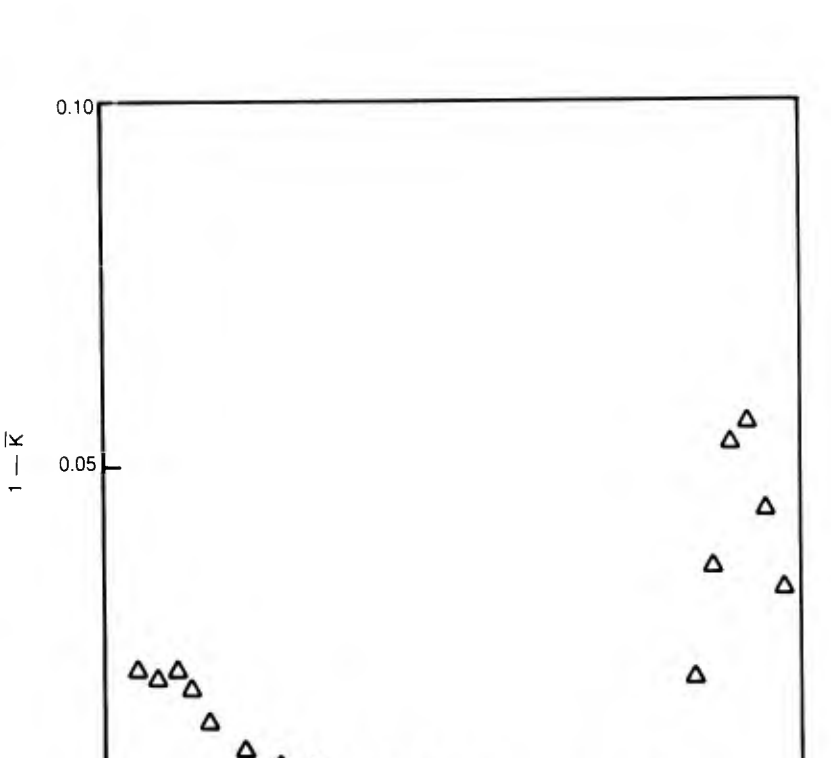

Figure 12 Two Stage Compressor, Second Stage Rotor, Blockage, ϕ = 0.51

DISCUSSION

Ph.Ramette, Fr

In Figure 8, which gives the total pressure losses for the second stage rotor of the two-stage compressor, the total pressure loss is close to zero near the hub, because of the high total pressure fluid moving towards the hub near the pressure surface side of the blade wake, as you said. In the midspan region, the negative loss could be due to the large tip clearance, which is 4%, so that the flow near the tip of the blades is moving toward midspan at the exit of the rotor, redistributing the radial total pressure profile. Could you comment about this?

Author's Reply

As mentioned in the paper, aside from small measurement errors, the two prime candidates for explaining the negative loss at the midspan of the second stage rotor are radial redistribution of high and low total pressure fluid and radial displacement of the axisymmetric stream surface. Both of these possibilities could be accentuated by the very large tip clearance. This question may become clearer as we examine additional data.

B.Lakshminarayana

(1) I would like to congratulate you on a large amount of fine data.

(2) The thick boundary layer case had very small velocity gradients near the wall and had almost a linear profile from hub to mid-radius. Since the secondary flow is very sensitive to the velocity gradients, rather than the thickness, it is not surprising that the thick boundary layer case did not have severe secondary flow. It would be useful to generate a thick boundary layer with steep velocity gradients near the wall.

Author's Reply

The thin and thick inlet C_x profiles in the isolated rotor tests were very similar in terms of their shape factors (H = 1.3 and 1.5 respectively). Since to a first approximation the secondary flow process varies linearly with the initial streamwise and normal components of vorticity the factor of 4 variation in inlet boundary layer thickness was felt to be a fairly significant variation. Finally, the two-stage test lends strong evidence that secondary flow will in general be relatively weak, particularly in comparison with the effects of corner stall.

C.L.Ball, US

My comment is not made in terms of trying to generalize between your results and that which we noted in the two-stage fan, but it is interesting to note that the circumferential blockage near the walls behind the low speed rotor is higher than in the core flow region, which is further evidence of the highly non-axisymmetric flows in the endwall boundary layer region as compared to free stream, as we observed behind the stators in the two-stage fan.

Author's Reply

I agree. Our data on these and other tests have indicated that the flow in the endwall regions is in general far more non-axisymmetric than the flow in the midspan region.

Ch.Hirsch, Be

I would like, first of all, to congratulate the authors for their continuous effort in the production of such high quality data.

I am very pleased by the importance given to the concept of tangential blockage distinct from the end-wall blockage. We are using this distinction in our through-flow calculation method and connect the blockage K to the local loss coefficient through the momentum thickness of the wake. Therefore it is not surprising that the variation of K is similar to the variation of the total pressure loss. Actually we think that the variation could be deduced from the other. Have you tried to derive the variation of K from the radial variation of wake thickness?

Author's Reply

As we noted in the paper, "the blockage profiles bear a qualitative similarity to the loss profiles". To date, however, we have not attempted to quantify this relationship. This will definitely be something to look into as we evaluate the rest of our data.

J.Moore, US

(1) Is the ammonia neutrally buoyant in these flows?

(2) Is there enough shear work at the shroud, combined with secondary flow from the shroud to cause the local increases in rotary total pressure which you observe?

Author's Reply

Strictly speaking, the ammonia used in the flow visualization is not neutrally buoyant but we believe that it does accurately follow the surface streamlines. This belief is based on numerous previous tests where density ratio and blowing rate effects were demonstrated to have no noticeable impact on the indicated surface streamline direction.

The increase in rotary total pressure was observed primarily on the two-stage compressor second stage rotor in the midspan region and very close to the hub (Fig.8). From Figure 6 it is difficult to see how shear work and secondary flow at the shroud could influence the rotary total pressure of the midspan and hub fluid other than by radial displacement of the axisymmetric stream surfaces due to blockage at the tip. The flow visualization (Fig.3) also suggests that it is unlikely that fluid originating at the rotor shroud could find its way radially into the midspan region.